molecular pharmaceutics

pubs.acs.org/molecularpharmaceutics

Article

[^{18}F]Atorvastatin Pharmacokinetics and Biodistribution in Healthy Female and Male Rats

Gonçalo S. Clemente, Inês F. Antunes, Jürgen W. A. Sijbesma, Aren van Waarde, Adriaan A. Lammertsma, Alexander Dömling, and Philip H. Elsinga*

Cite This: *Mol. Pharmaceutics* 2021, 18, 3378−3386

Read Online

ACCESS | Metrics & More | Article Recommendations

ABSTRACT: Statins are 3-hydroxy-3-methylglutaryl-coenzyme A reductase inhibitors that are widely used to prevent cardiovascular diseases. However, a series of pleiotropic mechanisms have been associated with statins, particularly with atorvastatin. Therefore, the assessment of [^{18}F]atorvastatin kinetics with positron emission tomography (PET) may elucidate the mechanism of action of statins and the impact of sexual dimorphism, which is one of the most debated interindividual variations influencing the therapeutic efficacy. [^{18}F]Atorvastatin was synthesized via a previously optimized ^{18}F-deoxyfluorination strategy, used for preclinical PET studies in female and male Wistar rats (n = 7 for both groups), and for subsequent *ex vivo* biodistribution assessment. PET data were fitted to several pharmacokinetic models, which allowed for estimating relevant kinetic parameters. Both PET imaging and biodistribution studies showed negligible uptake of [^{18}F]atorvastatin in all tissues compared with the primary target organ (liver), excretory pathways (kidneys and small intestine), and stomach. Uptake of [^{18}F]atorvastatin was 38 ± 3% higher in the female liver than in the male liver. The irreversible 2-tissue compartment model showed the best fit to describe [^{18}F]atorvastatin kinetics in the liver. A strong correlation (R^2 > 0.93) between quantitative K_i (the radiotracer's unidirectional net rate of influx between compartments) and semi-quantitative liver's SUV (standard uptake value), measured between 40 to 90 min, showed potential to use the latter parameter, which circumvents the need for blood sampling as a surrogate of K_i for monitoring [^{18}F]atorvastatin uptake. Preclinical assays showed faster uptake and clearance for female rats compared to males, seemingly related to a higher efficiency for exchanges between the arterial input and the hepatic tissue. Due to the slow [^{18}F]atorvastatin kinetics, equilibrium between the liver and plasma concentration was not reached during the time frame studied, making it difficult to obtain sufficient and accurate kinetic information to quantitatively characterize the radiotracer pharmacokinetics over time. Nevertheless, the reported results suggest that the SUV can potentially be used as a simplified measure, provided all scans are performed at the same time point. Preclinical PET-studies with [^{18}F]atorvastatin showed faster uptake and clearance in female compared to male rats, apparently related to higher efficiency for exchange between arterial blood and hepatic tissue.

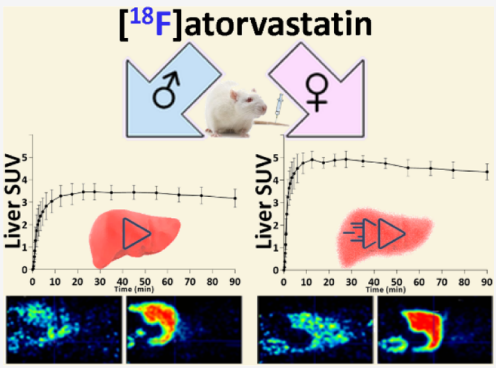

KEYWORDS: *fluorine-18, positron emission tomography (PET), atorvastatin, sexual dimorphism, pharmacokinetics*

INTRODUCTION

Statins are one of the most successful classes of drugs worldwide and are used to treat hypercholesterolemia and prevent atherosclerosis by binding and reversibly inhibiting 3-hydroxy-3-methylglutaryl-coenzyme A (HMG-CoA) reductase. Besides, statins are believed to have pleiotropic actions independent of their HMG-CoA reductase inhibition, being increasingly recognized to have additional protective mechanisms, such as anti-inflammatory, antiproliferative, immunomodulatory, and neuroprotective effects.[1,2] However, there is also a well-documented, but poorly understood, resistance or insufficient response to statin treatment among some patients.[3] This resistance or insufficient response is mostly linked to statin-associated muscle symptoms, although more serious side effects have occurred.[4] One of the most debated interindividual variations that arguably contribute to the pharmacokinetic and pharmacodynamic differences concerning the efficacy and toxicity of statins is sexual dimorphism.[5−7] It is known that there are sex-related differences in the metabolism of some drugs, which can be related to differences in the expression of receptors, enzymes, or transporter proteins that determine the

Received: April 15, 2021
Revised: July 21, 2021
Accepted: July 21, 2021
Published: August 5, 2021

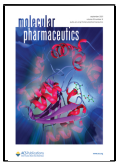

https://doi.org/10.1021/acs.molpharmaceut.1c00305
Mol. Pharmaceutics 2021, 18, 3378−3386

access of the drug to the target or the secretion of the metabolites formed.[8−11] Nevertheless, a real-time *in vivo* observation of the pharmacokinetics of statins in subjects of different sexes has not yet been attained.

Positron emission tomography (PET) is a well-established molecular imaging modality used in the clinic to diagnose several diseases. In addition, PET allows for assessing the efficacy of therapy and for demonstrating target engagement of a drug. Thus, PET has become increasingly relevant during the developmental stages of new drugs and in clarifying the mechanisms of action of existing drugs.[12]

An essential feature for the potency of modern statins is the presence of a fluorophenyl group that enables additional polar interactions and tighter binding to HMG-CoA reductase.[13] Replacing a stable fluorine atom by its radioisotope is not always straightforward, especially when it is located in electron-rich arenes that are not amenable to aromatic nucleophilic substitution, as in the case of statins. We previously reported that either Cu-mediated ^{18}F-fluorodeboronation[14] or Ru-mediated ^{18}F-deoxyfluorination[15] approaches can be used to synthesize a radiolabeled analog of atorvastatin, with the latter strategy providing far superior and reliable radiochemical yields (2% *vs* 20%). Atorvastatin is one of the most potent statins synthesized to date, being a standard treatment for primary and secondary prevention of cardiovascular diseases.[16,17] Atorvastatin also seems to have a particular propensity for pleiotropic effects, which may be related to its lipophilicity.[18−20] Preliminary *in vitro* evaluations from our group[15] showed that [^{18}F]atorvastatin retains the specific binding to HMG-CoA reductase of the conventional drug and shows increased uptake in atherosclerotic plaques (approx. 2:1) with respect to healthy vascular tissues. Therefore, [^{18}F]atorvastatin was administered for the first time to healthy male and female rats to enable *in vivo* identification of target activity sites and assess potential pharmacokinetic differences between the sexes.

EXPERIMENTAL SECTION

General Information. All chemicals and solvents were purchased from commercial suppliers of analytical grade and used without further purification. Aqueous [^{18}F]fluoride used in this work was produced by the ^{18}O(p,n)^{18}F nuclear reaction using an IBA (Ottignies-Louvain-la-Neuve, Belgium) Cyclone 18/18 cyclotron. [^{18}F]Atorvastatin was synthesized via Ru-mediated ^{18}F-deoxyfluorination in a Synthra GmbH RNplus modular radiosynthesizer (Hamburg, Germany), and identity, purity, and molar activity of the final product were assessed by ultraperformance liquid chromatography (UPLC) with a Waters ACQUITY HSS T3 column (1.8 μm 3.0 × 50 mm), a UV (λ = 254 nm), and a gamma radiation detector, as described below.

Synthesis of [^{18}F]Atorvastatin. [^{18}F]Atorvastatin was synthesized from a Ru-coordinated atorvastatin-derived precursor by ^{18}F-deoxyfluorination, as reported previously.[15] In summary, [^{18}F]fluoride was loaded onto a Chromafix 45-PS-HCO_3^- anion exchange cartridge, briefly dried under a helium stream, and slowly eluted to the reactor vial with a solution of the Ru-coordinated labeling precursor (2.5 μmol) and *N*,*N*-bis(2,6-diisopropylphenyl-1-chloroimidazolium chloride) (6.0 equiv) in methanol/dimethyl sulfoxide (DMSO) (1:3 v/v, 0.4 mL). The reaction mixture was left to stir for 30 min at 140 °C. After ^{18}F-deoxyfluorination, the ketal and *tert*-butyl protecting groups at the dihydroxyheptenoic acid side chains were removed by sequentially treating the reaction mixture with 1 mL of methanol/HCl 6 M (49:1 v/v) at 60 °C for 5 min, and 0.5 mL of methanol/aqueous NaOH 50% (9:1 v/v) for an extra 5 min at 60 °C. The full content of the reactor vial was then loaded onto a semi-preparative high-performance liquid chromatography (HPLC) column to purify [^{18}F]-atorvastatin. The HPLC system used a SymmetryPrep C18 7 μm 7.8 × 300 mm column as stationary-phase and a combination of two solvents for the mobile-phase (A, sodium acetate 0.05 M pH 4.7; B, acetonitrile). Solvent gradient was as follows: 0−4 min, 90% A; 4−15 min, 90% A to 20% A; 15−25 min, 20% A to 5% A; 25−33 min, 5% A; 33−34 min, 5% A to 90% A; 34−35 min, 90% A; flow, 6 mL·min^{-1}; $R_t \approx 16$ min. Finally, solid-phase extraction allowed for the exchange of solvents, and [^{18}F]atorvastatin was obtained in a physiological and injectable calcium acetate solution[15] (0.05 M pH 7.0) in <10% ethanol.

PET Imaging and Blood Sampling. All animal procedures were carried out following the European Union directives for animal experiments (86/609/CEE, 2003/65/CE, and 2010/63/EU), and the protocols used (AVD105002015166/IvD15166-01-006) were previously approved by the Dutch National Committee on Animal Experiments and the Institutional Animal Care and User Committee of the University of Groningen. Female and male Wistar RjHan:WI albino rats (8 weeks old) were purchased from Janvier Laboratories (Le Genest-Saint-Isle, France). The animals were quarantined for 1 week, provided with standard chow and water *ad libitum* and housed under temperature-, light-, and sound-controlled conditions.

As the bioavailability and metabolism of statins are affected by hepatic drug-metabolizing enzymes, which have sex-dependent expressions,[21] a group of female (n = 7) and male rats (n = 7) were included. Age-matched animal groups (9−10 weeks at the time of scan) were used, instead of body-weight matched, based on the known significant effect of age on the metabolic activity of the liver in rats. Moreover, the liver-weight/body-weight ratio between male and female Wistar rats of the same age generally remains constant.[22]

For the preclinical PET scans, Wistar rats (females: 239.3 ± 7.5 g, n = 7; males: 403.9 ± 13.6 g, n = 7) were anesthetized with isoflurane (5% for induction and 2% for maintenance), and the femoral artery was cannulated to facilitate access for blood sampling. A micro-PET Focus 220 system (Siemens Medical Solution Inc.) was used for all experiments. The animals were placed on the scanner table in a prone position on top of a heating pad at 38 °C, with the torso in the field of view. After positioning, they were monitored continuously for temperature and oxygen saturation levels. First, a 10 min transmission scan with a ^{57}Co point source was acquired for the purpose of scattering and attenuation corrections. Simultaneously with the start of the subsequent emission scan, [^{18}F]atorvastatin (radiochemical purity: >99%; molar activity: 80.5 ± 27.6 GBq·μmol^{-1}) was administered as a single bolus over 1 min (1 mL·min^{-1}) using a Harvard infusion pump via the tail vein (effective injected dose: 24.8 ± 5.9 MBq; estimated molar mass injected: 340 ± 151 pmol).

All emission scans were acquired in list mode for 90 min. Blood samples were taken 10, 20, 30, 40, and 50 s and 1, 1.5, 2, 3, 5, 7.5, 10, 15, 30, 60, and 90 min after tracer injection to determine the total activity concentration of radiotracer in whole blood and plasma (arterial input function). A maximum of 1.5 mL of blood was sampled from each rat, which does not exceed 10% of the total circulating blood volume (approx-

https://doi.org/10.1021/acs.molpharmaceut.1c00305
Mol. Pharmaceutics 2021, 18, 3378−3386

imately 64 mL·kg^{-1}). The drawn blood was replaced by a heparinized saline solution. Part of each blood sample was reserved and centrifuged (6000 rpm for 3 min in a Hettich MIKRO 20 centrifuge) to separate the plasma fraction. The radioactivity in each whole blood and plasma sample was measured with a gamma-counter (PerkinElmer Wallac Wizard 1470), and corrected for volume and decay (no correction was made for the presence of radioactive metabolites as these were never observed over time), and plotted as a function of time.

The amount of radioactivity in the blood and plasma samples was then normalized to body weight and injected dose to calculate standardized uptake values {SUV = tissue activity concentration [MBq/g]·[injected dose (MBq)/rat body weight (g)]$^{-1}$}.

***Ex Vivo* Biodistribution and Radiometabolite Analysis.** After scanning, the animals were euthanized by heart excision while under deep anesthesia, and organs were harvested and weighed. Due to the structural and metabolic heterogeneity of the rat liver, a section of the middle lobe was collected to assess biodistribution. The radioactivity in each organ was determined with a PerkinElmer Wallac Wizard 1470 gamma-counter to assess biodistribution (SUV).

The metabolic stability of [^{18}F]atorvastatin was assessed either by two distinct silica-gel thin layer chromatography (TLC-SG) systems or by UPLC for each blood and plasma sample and additionally, for urine, feces, and liver homogenate samples collected during organ harvesting. Aliquots of the blood samples were directly analyzed by radio-TLC without further treatment or dilution. The remaining volume of the blood samples (approx. 0.1 mL) was centrifuged (6000 rpm for 3 min in a Hettich Universal 320R centrifuge) to separate the plasma fraction. Plasma was directly analyzed by radio-TLC without further treatment or dilution and by radio-TLC and radio-UPLC after protein precipitation with three volumes of acetonitrile (typically 15 μL for 5 μL of plasma) and separation of the pellet (6000 rpm for 5 min in a Hettich MIKRO 20 centrifuge); 15 ± 2% of [^{18}F]atorvastatin trapped in the pellet. Urine was directly analyzed by radio-TLC and radio-HPLC without further treatment or dilution. Feces and liver samples were dipped in a solution of tris−HCl (0.05 M, pH 7.4)/ethanol (1:1), homogenized with a Heidolph DIAX 600 homogenizer, centrifuged for 5 min (5000 rpm in a Thermo Scientific Heraeus Labofuge 200 centrifuge), and left to rest. Aliquots of the feces and liver homogenates were directly analyzed by radio-TLC. TLC-SG developed with ethanol/sodium phosphate 0.1 M pH 7.4 (65:35 v/v) has R_f([^{18}F]F$^-$) ≈ 0.0−0.1, R_f([$^{19/18}$F]atorvastatin) ≈ 0.8, and R_f(atorvastatin lactone) ≈ 1.0). TLC-SG developed with a mixture of chloroform, methanol, toluene, and ammonia (5:2:1:0.2 v/v/v/v) has R_f([^{18}F]F$^-$) ≈ 0.0−0.1, R_f([$^{19/18}$F]atorvastatin) ≈ 0.4, and R_f(atorvastatin lactone) ≈ 0.8). The UPLC system used a Waters ACQUITY HSS T3 1.8 μm 3.0 × 50 mm column as a stationary phase and a combination of two solvents for the mobile phase (A, sodium acetate 0.01 M/MeOH/ACN 9:0.6:0.4 v/v/v; B, sodium acetate 0.01 M/MeOH/ACN 1:5.4:3.6 v/v/v). The solvent gradient was as follows: 0−2 min, 100% A; 2−5 min, 100% A to 40% A; 5−6 min, 40% A to 0% A; 6−9 min, 0% A; 9−10 min, 0% A to 100% A; flow, 0.8 mL·min^{-1}. UPLC retention times were R_t([^{18}F]F$^-$) ≈ 0.5 min, R_t([$^{19/18}$F]atorvastatin) ≈ 6.5 min, and R_t(atorvastatin lactone) ≈ 7 min.

Reconstruction of PET Images and Pharmacokinetic Modeling. List mode data of the emission scans were rebinned into 24 successive frames (6 × 10, 4 × 30, 2 × 60, 1 × 120, 1 × 180, 4 × 300, and 6 × 600 s). All frames were reconstructed using an iterative algorithm (OSEM2d, 4 iterations, 16 subsets) after being normalized and corrected for attenuation, random coincidences, scatter and radioactive decay. A three-dimensional volume of interest (VOI) was manually drawn by a single observer on the summed images, delineating the desired area on the summed PET images (0−90 min) using the PMOD software package (version 4.103; PMOD Technologies LLC). These VOIs were used to generate corresponding time−activity curves (TACs) corrected for time, injected dose, and body weight and to calculate the SUV of each of the 24 frames.

As atorvastatin is known to reversibly bind to HMG-CoA reductase in the liver,[23] two reversible compartment models (1- and 2-tissue compartment models) were used to fit the liver TACs. However, although binding to HMG-CoA is reversible, atorvastatin is a drug with a long residence time to increase its cholesterol-lowering efficacy,[24] and therefore it may act as an irreversible tracer within the time frame of a PET scan. Thus, an irreversible 2-tissue compartment model was also tested to identify the model that best describes [^{18}F]atorvastatin kinetics. Therefore, using individually measured whole blood and plasma input functions, generated tissue TACs were fitted to reversible 1- and 2-tissue compartment models (eqs 1 and 2) and irreversible 2-tissue compartment models (eq 3). Additionally, liver-to-plasma concentration ratios over the scanning time were plotted.

$$\frac{dC_1(t)}{dt} = K_1 C_p(t) - k_2 C_1(t) \tag{1}$$

$$\frac{dC_1(t)}{dt} = K_1 C_p(t) - (k_2 + k_3) C_1(t) + k_4 C_2(t)$$
$$\frac{dC_2(t)}{dt} = k_3 C_1(t) - k_4(t) \tag{2}$$

$$\frac{dC_1(t)}{dt} = K_1 C_p(t) - (k_2 + k_3) C_1(t)$$
$$\frac{dC_2(t)}{dt} = k_3 C_1(t) \tag{3}$$

The used kinetic models allowed for an estimation of the rate constants (K_1, k_2, k_3, and k_4) between compartments (C_p, C_1, and C_2), the total volume of distribution ($V_T = K_1/k_2 \cdot [1 + (k_3/k_4) + \nu_b]$) for reversible models, and the unidirectional net rate of influx ($K_i = K_1 k_3/[k_2 + k_3]$) for the irreversible model (Figure 1).

No reference tissue models were considered, as all tissues express HMG-CoA reductase,[25−27] thereby precluding the definition of a region with no specific binding. The correction for the fractional blood volume (V_b) in the hepatic tissue was disabled from fitting (*i.e.*, the software's default setting $V_b = 0$ was used) because preliminary attempts to use either a fixed (from 3 to 21%) or a fluctuating value invariably led to higher and more inconsistent AIC values and poorer fits. This inconsistency may be related to an expected heterogeneity between the hepatic function of different individuals. Therefore, a simplified approach with no blood volume correction was chosen. The most appropriate compartment model for [^{18}F]atorvastatin was selected by taking into consideration the Akaike information criterion (AIC, a lower value for best fit)

https://doi.org/10.1021/acs.molpharmaceut.1c00305
Mol. Pharmaceutics 2021, 18, 3378−3386

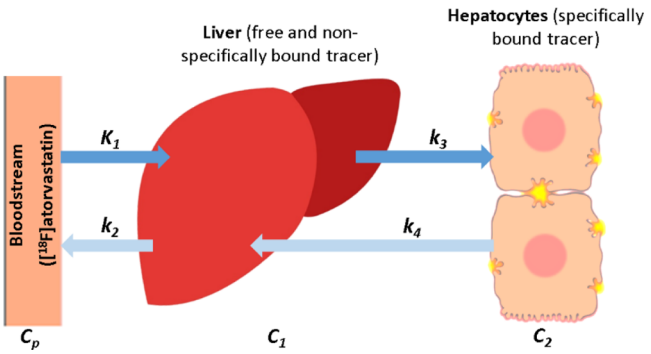

Figure 1. Representative scheme of the pharmacokinetic compartments regarded and respective exchange rate constants.

and the lowest standard error (SE %) associated with the V_T and K_i kinetic parameters.

The elimination half-life of [^{18}F]atorvastatin from the liver was estimated by fitting a single exponential curve to the TAC data from 27.5 min using an iterative nonlinear least square approach in GraphPad software. The plasma elimination half-life was estimated with the same approach but using the plasma SUV data from 1 min after intravenous injection.

Statistical Analysis. Data are expressed as mean ± standard deviation (SD). Unpaired two-tailed *t*-tests were used for statistical evaluations. A $p < 0.05$ was considered statistically significant ($*p < 0.05$; $**p < 0.02$; $***p < 0.001$). Statistical analyses of data were performed using GraphPad Prism version 6.01 for Windows (GraphPad Software, La Jolla, CA, USA).

RESULTS

[^{18}F]Atorvastatin Synthesis. [^{18}F]Atorvastatin was obtained within a synthesis time of approximately 80 min and with a final radiochemical yield of 26 ± 5% (decay corrected from the beginning of synthesis). The radiochemical purity was always higher than 99%, and the average molar activity was 80.5 ± 27.6 GBq·μmol^{-1}.

Biodistribution, Radiometabolite Analysis, and Arterial Input Function Kinetics. The *ex vivo* biodistribution at approximately 120 min after intravenous administration of [^{18}F]atorvastatin (Table 1) showed statistically significant differences between females and males in the kidney and gonads ($p < 0.05$).

The search for potential products of [^{18}F]atorvastatin defluorination or metabolism in blood, plasma, urine, feces, and liver homogenate samples invariably showed the absence of radiochemical species beyond parent [^{18}F]atorvastatin both in females and in males (Figure 2). As no radiolabeled metabolites or defluorination products were detectable in blood and plasma, there was no need to correct the [^{18}F]atorvastatin arterial input function.

Because [^{18}F]atorvastatin was administered as a single bolus over 1 min (1 mL·min^{-1}), the blood concentration reached a peak approximately 55 s after the start of injection (Figure 3), with a non-significantly different blood clearance half-life of 41 ± 9 and 53 ± 16 s for females and males, respectively. Besides, no significant differences were seen between female and male [^{18}F]atorvastatin concentrations in whole blood and plasma at any time point, nor in the areas under the curve (AUC).

PET Images and TACs Generation. In agreement with the biodistribution data, PET images (Figure 4) showed negligible uptake of [^{18}F]atorvastatin in all tissues compared with the primary target organ (liver), excretory pathways (kidneys and small intestine), and stomach.

TACs confirmed a significantly higher [^{18}F]atorvastatin uptake in females compared with male hepatic tissues at all times (Figure 5). After reaching a plateau, the uptake in the female liver was 38 ± 3% higher than that in the male liver. This difference was statistically significant ($p < 0.001$) during the entire 2.5−90 min interval. As expected, based on the primary target organ and lipophilic nature of atorvastatin, the excretion route was mostly hepatic, whereas the renal pathway was of minor importance. Liver elimination half-lives were

Table 1. *Ex Vivo* Biodistribution of [^{18}F]Atorvastatin in Rats, Approx. 2 h after Administration[a]

	SUV (n = 7)		tissue-to-plasma ratios (n = 7)	
tissues	females average ± SD	males average ± SD	females	males
heart	0.048 ± 0.014	0.067 ± 0.019	1.315 ± 0.188	1.441 ± 0.229
lungs	0.142 ± 0.047	0.139 ± 0.042	3.996 ± 1.060	3.026 ± 0.665
liver	10.556 ± 2.715	11.719 ± 1.935	294.498 ± 78.744	252.605 ± 78.521
spleen	0.059 ± 0.010	0.081 ± 0.019	1.573 ± 0.437	1.743 ± 0.415
pancreas	0.041 ± 0.007	0.067 ± 0.033	1.106 ± 0.298	1.570 ± 0.611
kidney	0.771 ± 0.279*	0.583 ± 0.200*	23.442 ± 10.222*	12.972 ± 3.335*
stomach wall	1.646 ± 0.832	1.848 ± 0.975	51.986 ± 33.076	44.424 ± 24.600
small intestine wall	0.215 ± 0.052	0.258 ± 0.130	6.314 ± 2.681	5.656 ± 1.924
large intestine wall	0.052 ± 0.036	0.072 ± 0.029	1.678 ± 1.124	1.751 ± 0.817
urinary bladder wall	0.068 ± 0.056	0.111 ± 0.095	2.409 ± 2.032	3.142 ± 3.028
muscle	0.018 ± 0.004	0.029 ± 0.011	0.480 ± 0.048*	0.666 ± 0.200*
fat	0.022 ± 0.007	0.044 ± 0.027	0.656 ± 0.223	1.161 ± 0.876
bone	0.023 ± 0.011	0.036 ± 0.008	0.661 ± 0.312	0.792 ± 0.254
bone marrow	0.124 ± 0.050	0.134 ± 0.060	3.724 ± 1.818	3.100 ± 1.111
ovaries/testes	0.063 ± 0.022**	0.018 ± 0.005**	1.897 ± 0.881**	0.400 ± 0.158**
brain	0.006 ± 0.003	0.015 ± 0.013	0.190 ± 0.070	0.425 ± 0.403
whole blood	0.053 ± 0.037	0.044 ± 0.011	1.673 ± 1.073	0.945 ± 0.179
plasma	0.037 ± 0.009	0.046 ± 0.015		

[a] $*p < 0.05$; $**p < 0.02$.

https://doi.org/10.1021/acs.molpharmaceut.1c00305
Mol. Pharmaceutics 2021, 18, 3378−3386

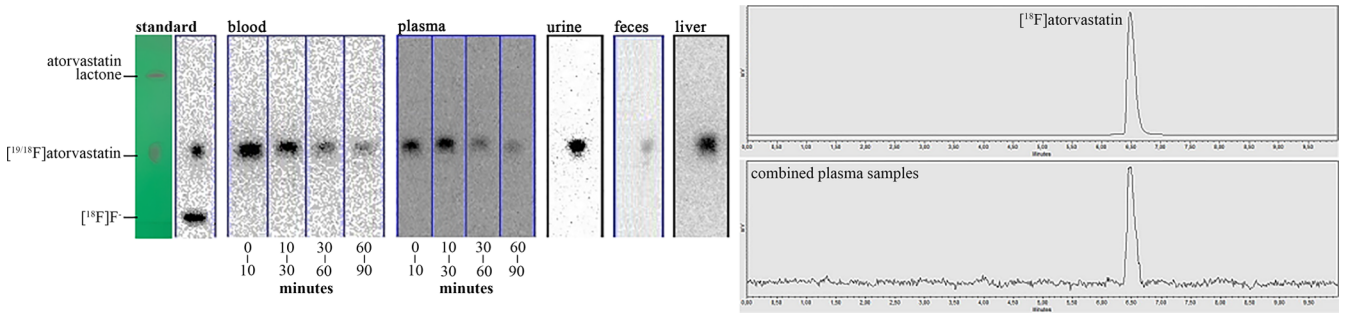

Figure 2. Representative profiles of the radiometabolites in blood, plasma, urine, feces, and liver.

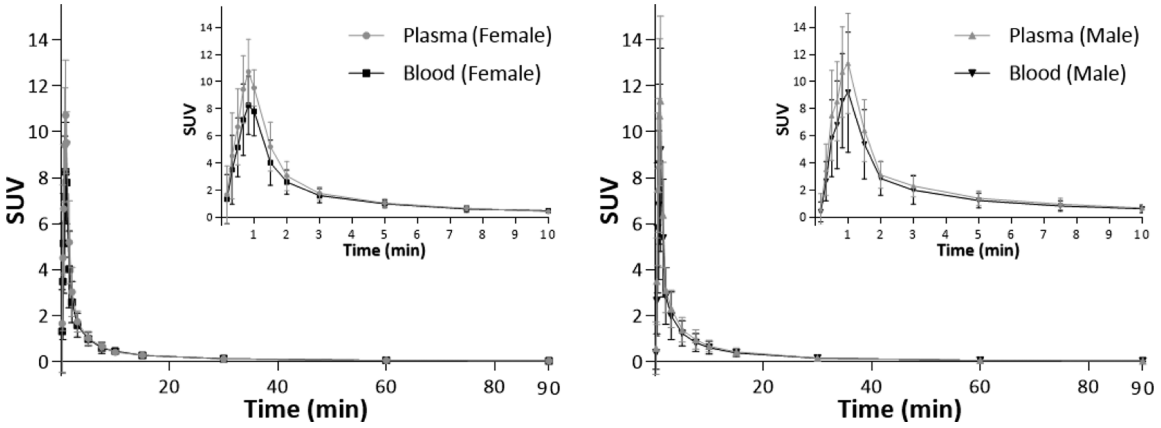

Figure 3. [18F]Atorvastatin arterial input functions in female (left) and male (right) rats (n = 7 for each group).

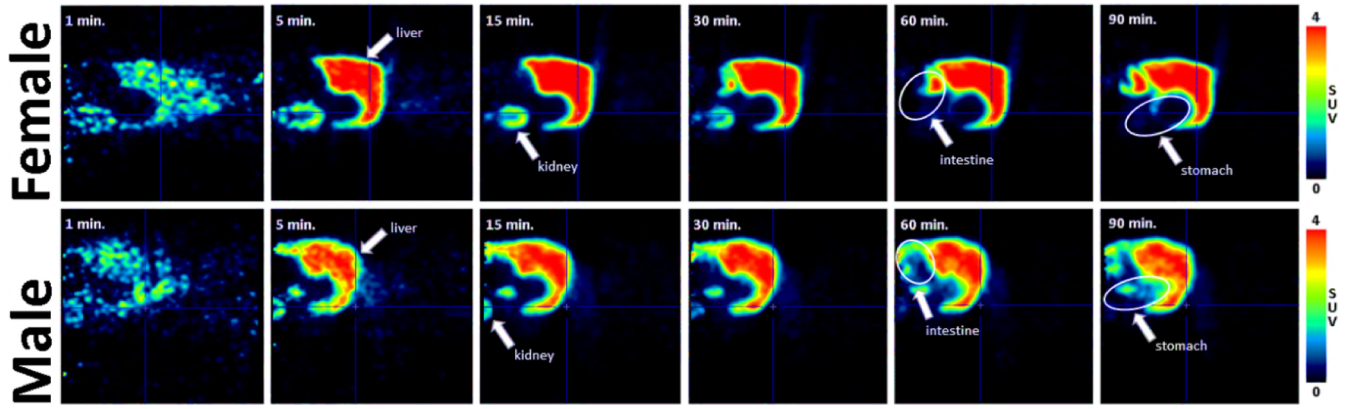

Figure 4. Representative maximum intensity sagittal projection images of female (top) and male (bottom) rat abdominal regions at different times after administration of [18F]atorvastatin.

approximately 4.5 h for females and 6.5 h for males. However, because data points were only available for 60 min, the determination of such long half-lives is prone to error.

Kinetic Modeling. Plotting the liver-to-plasma ratio of [18F]atorvastatin concentrations as a function of time (Figure 6) is a straightforward way to evaluate whether and, if so, when equilibrium is reached. The continuous increase of this plot shows that equilibrium is not being reached within the 90 min scanning interval.

When considering the individual AIC and its overall SD values estimated with the PMOD kinetic tool, both reversible and irreversible 2-tissue compartment models seem to be similarly able to describe the hepatic kinetics of [18F]-atorvastatin (Figure 7). However, the predictive power of the reversible 2-tissue compartment model comes at the cost of additional parameters, particularly k_4, whose results tend to be equal to zero, and very significant individual standard errors (SE % > 10, Table 2). Therefore, the more simplified kinetic model, the irreversible 2-tissue compartment model, was selected to describe the overall hepatic kinetics of [18F]-atorvastatin and estimate the net rate of influx (K_i). For the irreversible 2-tissue compartment model, K_i values were significantly different between female and male rats (p = 0.0017). As K_i depends on K_1, k_2, k_3, and k_4, and of these microparameters, only K_1 was significantly different between female and male rats (p = 0.0002); the increase in female's K_i seems to be fully explained by an increase in K_1 (Table 2).

Quantitative K_i and semiquantitative SUV were correlated to evaluate the potential of using the latter parameter, which has the advantage of circumventing the need for blood sampling, as

https://doi.org/10.1021/acs.molpharmaceut.1c00305
Mol. Pharmaceutics 2021, 18, 3378−3386

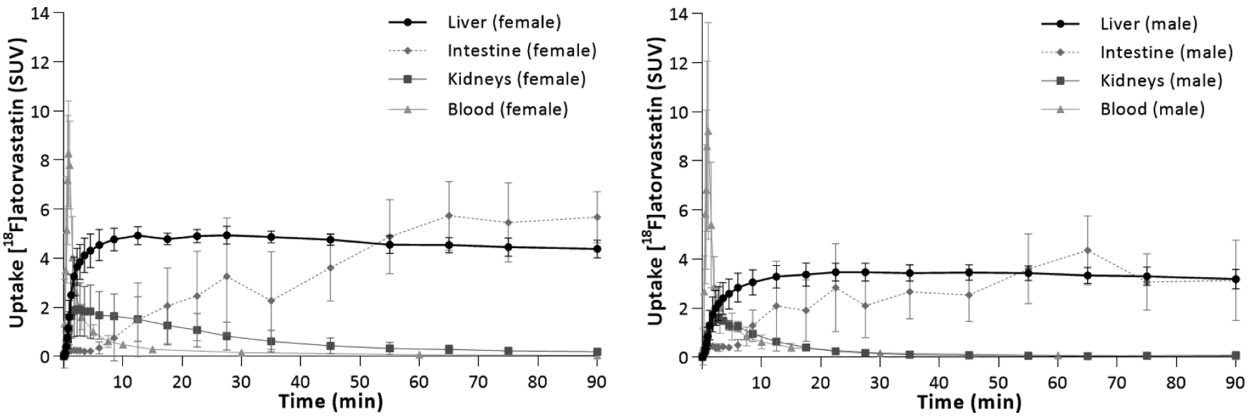

Figure 5. [^{18}F]Atorvastatin uptake (SUV) over time in female (left) and male (right) rats (n = 7 for each group).

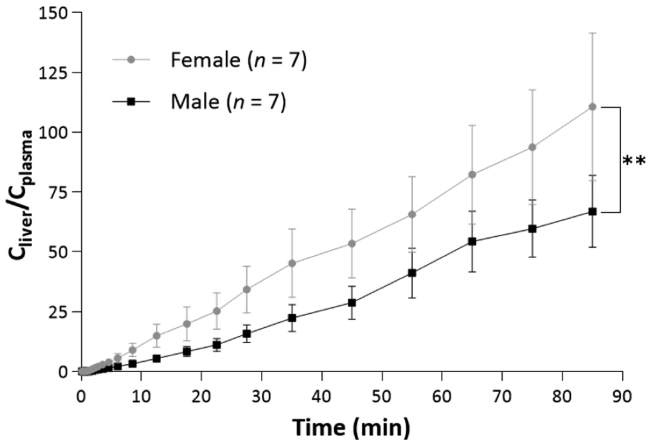

Figure 6. Liver-to-plasma concentration ratio of [^{18}F]atorvastatin in female and male rats over time (n = 7 for each group).

a surrogate of K_i for monitoring [^{18}F]atorvastatin uptake. The liver SUV average (from the 40 to 90 min plateau, where the SD was minimal) of each PET scan was correlated with the corresponding K_i values (Figure 8).

DISCUSSION

Both PET and biodistribution studies confirmed an extensive liver uptake of [^{18}F]atorvastatin in healthy rats, a known characteristic of all statins.[28] More importantly, no off-target accumulation was seen beyond hepatic tissues, which are the primary site of action for HMG-CoA reductase inhibitors. However, a hypothetic off-target accumulation, potentially leading to beneficial or negative pleiotropic effects, may be pathology-dependent (*e.g.*, sites of inflammation or cell proliferation), induced by a therapeutic (and not a tracer) dose, or occur as a downstream consequence of liver metabolism. Further studies will be needed to unravel the poorly understood pleiotropic effects of statins, and [^{18}F]-atorvastatin may be a useful tool to enable the design of specific *in vitro* and *in vivo* assays. Apart from the liver and excretory organs, the stomach wall was the only structure showing reasonable [^{18}F]atorvastatin uptake, which may be related to the high HMG-CoA reductase expression in the gastrointestinal tract.[25−27] This is the first time that accumulation of atorvastatin in the stomach wall was imaged *in vivo*, which may explain the reported gastric ulceration side effect of this drug, which appears to be less pronounced for other statins.[29] The propensity for this accumulation in the stomach observed with [^{18}F]atorvastatin will certainly be even more prominent when the HMG-CoA reductase inhibitor is administered orally. This finding is a clear example of how PET can detect drug accumulation in nontarget organs that may be associated with undesired side effects.

The presence of a negligible fraction of radiometabolites in blood and plasma is in agreement with what has been reported for other radiolabeled statins[30−32] and is in line with the known metabolic pathways of statins, which are extensively metabolized in the liver by glucuronidation and whose metabolites are eliminated by biliary secretion and directly excreted through the intestine.

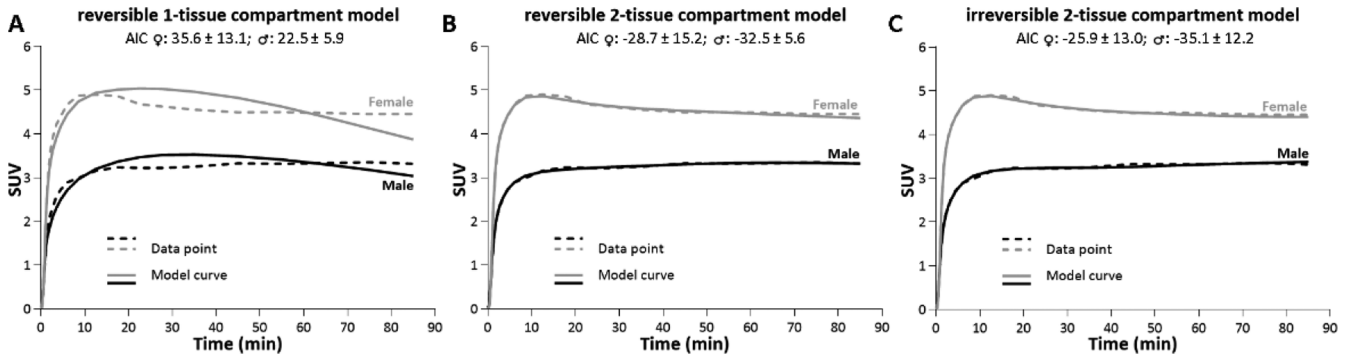

Figure 7. Representative fits of [^{18}F]atorvastatin liver TACs of female and male rats using (A) reversible 1-tissue compartment model and (B) reversible 2-tissue compartment model and (C) AIC for each group (n = 7).

https://doi.org/10.1021/acs.molpharmaceut.1c00305
Mol. Pharmaceutics 2021, 18, 3378−3386

Table 2. Kinetic Parameters for Reversible and Irreversible 2-Tissue Compartment Models of [^{18}F]Atorvastatin in the Liver of Female and Male Rats (n = 7 for Each Group)[a]

	reversible 2-tissue compartment		irreversible 2-tissue compartment	
	female	male	female	male
K_1 (mL/cm^3/min)	0.298 ± 0.138	0.185 ± 0.034	0.327 ± 0.057***	0.180 ± 0.032***
SE % (K_1)	1.469 ± 0.675	1.421 ± 0.185	1.148 ± 0.316	0.987 ± 0.185
k_2 (min^{-1})	0.056 ± 0.028	0.038 ± 0.012	0.035 ± 0.014	0.025 ± 0.008
SE % (k_2)	11.784 ± 4.571	15.394 ± 5.476	6.831 ± 1.941	6.882 ± 2.017
k_3 (min^{-1})	0.071 ± 0.028	0.070 ± 0.020	0.033 ± 0.009	0.032 ± 0.011
SE % (k_3)	17.517 ± 7.943	23.520 ± 10.034	7.844 ± 2.651	8.413 ± 4.250
k_4 (min^{-1})	0.009 ± 0.004	0.011 ± 0.006		
SE % (k_4)	28.437 ± 18.713	32.197 ± 21.402		
V_T (mL/cm^3)	63.198 ± 24.024	44.008 ± 19.818		
SE % (V_T)	18.960 ± 14.019	20.736 ± 18.253		
K_i ($=K_1k_3/(k_2 + k_3)$)			0.162 ± 0.033**	0.100 ± 0.016**

[a]**p < 0.02; ***p < 0.001.

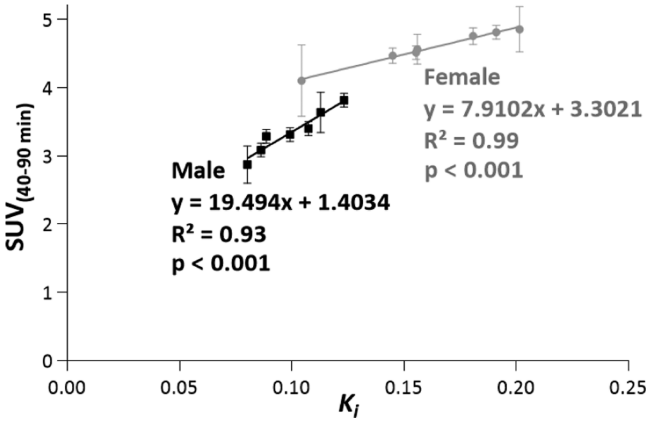

Figure 8. Correlation between [^{18}F]atorvastatin liver SUV and K_i derived using the irreversible 2-tissue compartment model (n = 7).

The [^{18}F]atorvastatin liver TACs revealed that rapid hepatic uptake occurred immediately after intravenous administration. Also, uptake was 38 ± 3% higher (p < 0.001) in the female liver than in the male liver. This uptake is followed by a radiotracer elimination half-life 20 to 30% faster (p < 0.02) from the female liver. These results are in line with those reported clinically in humans following oral atorvastatin treatment. The elimination of atorvastatin is approximately 20% faster in women than in men, and the maximum serum concentration in females is about 18% higher.[23] However, it is still unclear what mechanisms are behind this sexual dimorphism in atorvastatin pharmacokinetics, with differences in the membrane-bound transport protein expression (particularly, the organic anion transporters) or in the HMG-CoA reductase activity usually being the most frequently mentioned hypotheses.[23,33]

Within the time frame of the study (90 min), there was no appreciable washout, and the kinetic modeling showed an overall better fit of the irreversible 2-tissue compartment model to the PET acquired data. Using this kinetic model, the K_1, k_2, and k_3 kinetic microparameters were calculated. Only K_1 was significantly different between the female and male rats (p = 0.0002), which may explain the pharmacokinetic differences among sexes. This pharmacokinetic variance seems primarily related to a greater exchange efficiency from plasma to the liver because K_1 and K_1/k_2, but not k_2 and k_3, were significantly different between female and male rats (p < 0.05). Theoretically, these flux differences may be due to variations in the activity or expression of membrane transport proteins in the liver[23,33] (Table 3). As $K_i = K_1k_3/(k_2 + k_3)$, there is always a blood flow effect associated with the calculated kinetic parameters. Nevertheless, because k_3 is low, this effect is not expected to be prominent. In fact, if k_3 values were large (much larger than k_2), K_i would approximate to K_1, and [^{18}F]-atorvastatin would become a real flow tracer.

Table 3. Hepatic Reference Values and Cholesterol Levels for Adult Female and Male Rats

	female rats	male rats	refs
hepatic organic anion transporter expression	115 TPM	95 TPM	27
hepatic HMG-CoA reductase expression	31 TPM	17 TPM	27
hepatic LDL receptor expression	108 TPM	111 TPM	27
LDL serum levels	36.5 mg/dL	48.7 mg/dL	34
total cholesterol serum levels	118.3 mg/dL	115.8 mg/dL	34

Due to the slow [^{18}F]atorvastatin kinetics, no equilibrium was reached (Figure 6), which indicates that it is difficult to obtain sufficient kinetic information to accurately characterize the pharmacokinetics of the radiotracer with a 90 min scanning protocol (hence the relatively high SDs of the kinetic microparameters). Nevertheless, this may be mitigated if K_i provides sufficient and accurate information when compared to SUV.

Although we realize that the major blood input is derived from the portal vein, an arterial input was applied to estimate the liver input function. In our estimation, we consider that there is a dual blood supply. The second supply is somehow delayed compared to the first, but this should not affect the quantification of a "late" process, such as volume of distribution or rate of influx. This estimation may be problematic when there is significant binding in the gut. However, our biodistribution data show only a % ID/g of 0.09 ± 0.05 and 0.02 ± 0.01, for the small and large intestine, in the time window studied.

There was a strong correlation (R^2 > 0.93) between K_i and SUV measured between 40 and 90 min. Furthermore, the 38 ± 3% higher (p = 0.0016) SUV in the liver of females was correlate well with the predicted K_i values, which was 37 ± 14% higher (p = 0.0016) in the liver of females. These

https://doi.org/10.1021/acs.molpharmaceut.1c00305
Mol. Pharmaceutics 2021, 18, 3378−3386

observations suggest that SUV can potentially be used as a simplified measure, provided all scans are performed at the same time point. However, the feasibility of scans longer than 90 min should be explored in the future.

Further prolonged studies with [^{18}F]atorvastatin can confirm whether K_i values of late scans deviate from the K_i values obtained from a 90 min scan and provide additional evidence supporting or refuting the use of simpler SUV methods to evaluate the liver uptake of this radiotracer. In addition, future studies need to assess also whether the correlation between K_i and SUV remains the same under different conditions, especially after therapy, as therapy may change the radiotracer's clearance, which in turn would affect this correlation. The potential clinical implications resulting from the different relationship between SUV and K_i in females and males, apparently resulting from a dissimilar exchange efficiency from plasma to the liver, will also benefit from a more detailed study.

The different formulation and administration routes (parenteral *vs* enteral) and dose (tracer *vs* therapeutic amount) between radiolabeled and pharmacological atorvastatin will undeniably impact the overall absorption, distribution, metabolism, and excretion mechanisms. Furthermore, the possibility of species differences in the biodistribution and metabolism of atorvastatin should be carefully taken into account before extrapolating the results to humans. For example, a higher activity of the CYP3A enzymes (extensively involved in the metabolism of statins) has been reported in male rats compared to females, making the male rats potentially a closer model to what is expected in humans.[35] Nevertheless, the preclinical results presented here are important baseline findings for the design of further studies. [^{18}F]Atorvastatin showed potential to aid in assessing and understanding therapeutic-resistant cases and impacting patient selection for statin therapy, for example, by identifying high uptake in nontarget organs, assessing potentially inadequate clearance profiles, and evaluating specific uptake in atherosclerotic plaques.

CONCLUSIONS

Preclinical assays showed a faster uptake and clearance in female compared to male rats, apparently related to higher efficiency for exchange between arterial blood and hepatic tissue. However, the results herein reported with [^{18}F]-atorvastatin have to be carefully translated to the clinical setting where the drug is conventionally given orally. Therefore, it is still unclear whether these sex-related differences in the pharmacokinetics of [^{18}F]atorvastatin will be clinically relevant. A follow up of this work is evaluating [^{18}F]atorvastatin kinetics in humans (male and female, statin resistant and nonresistant patients, at baseline and after treatment) to assess whether PET scans can be predictive or not.

AUTHOR INFORMATION

Corresponding Author

Philip H. Elsinga − *Department of Nuclear Medicine and Molecular Imaging—University Medical Center Groningen, University of Groningen, 9713 GZ Groningen, The Netherlands;* orcid.org/0000-0002-3365-4305; Phone: +31-50-3613247; Email: p.h.elsinga@umcg.nl; Fax: +31-50-3611687

Authors

Gonçalo S. Clemente − *Department of Nuclear Medicine and Molecular Imaging—University Medical Center Groningen, University of Groningen, 9713 GZ Groningen, The Netherlands*

Inês F. Antunes − *Department of Nuclear Medicine and Molecular Imaging—University Medical Center Groningen, University of Groningen, 9713 GZ Groningen, The Netherlands;* orcid.org/0000-0002-8003-5291

Jürgen W. A. Sijbesma − *Department of Nuclear Medicine and Molecular Imaging—University Medical Center Groningen, University of Groningen, 9713 GZ Groningen, The Netherlands*

Aren van Waarde − *Department of Nuclear Medicine and Molecular Imaging—University Medical Center Groningen, University of Groningen, 9713 GZ Groningen, The Netherlands*

Adriaan A. Lammertsma − *Department of Nuclear Medicine and Molecular Imaging—University Medical Center Groningen, University of Groningen, 9713 GZ Groningen, The Netherlands*

Alexander Dömling − *Department of Drug Design, University of Groningen, 9713 AV Groningen, The Netherlands;* orcid.org/0000-0002-9923-8873

Complete contact information is available at: https://pubs.acs.org/10.1021/acs.molpharmaceut.1c00305

Notes

The authors declare no competing financial interest.

ACKNOWLEDGMENTS

The authors are grateful to the Ritter group at Max-Planck-Institut für Kohlenforschung to support the Ru-coordination chemistry.

ABBREVIATIONS

AIC, Akaike information criteria; AUC, area under curve; CYP3A, cytochrome P450, family 3, subfamily A; DMSO, dimethyl sulfoxide; HMG-CoA, 3-hydroxy-3-methylglutaryl-coenzyme A; HPLC, high-performance liquid chromatography; PET, positron emission tomography; SUV, standardized uptake value; TAC, time activity curve; TPM, transcripts per million; TLC, thin layer chromatography; UPLC, ultra high-performance liquid chromatography

REFERENCES

(1) Bedi, O.; Dhawan, V.; Sharma, P. L.; Kumar, P. Pleiotropic effects of statins: new therapeutic targets in drug design. *Naunyn-Schmiedeberg's Arch. Pharmacol.* **2016**, *389*, 695−712.

(2) Oesterle, A.; Laufs, U.; Liao, J. K. Pleiotropic Effects of Statins on the Cardiovascular System. *Circ. Res.* **2017**, *120*, 229−243.

(3) Reiner, Ž. Resistance and intolerance to statins. *Nutr., Metab. Cardiovasc. Dis.* **2014**, *24*, 1057−1066.

(4) Ward, N. C.; Watts, G. F.; Eckel, R. H. Statin Toxicity: Mechanistic Insights and Clinical Implications. *Circ. Res.* **2019**, *124*, 328−350.

(5) Taylor, F.; Ebrahim, S. Statins Work Just as Well in Women as in Men: Comment on "Statin Therapy in the Prevention of Recurrent Cardiovascular Events". *Arch. Intern. Med.* **2012**, *172*, 919−920.

(6) Cangemi, R.; Romiti, G. F.; Campolongo, G.; Ruscio, E.; Sciomer, S.; Gianfrilli, D.; Raparelli, V. Gender related differences in treatment and response to statins in primary and secondary cardiovascular prevention: The never-ending debate. *Pharmacol. Res.* **2017**, *117*, 148−155.

(7) Faubion, S. S.; Kapoor, E.; Moyer, A. M.; Hodis, H. N.; Miller, V. M. Statin therapy: does sex matter? *Menopause* **2019**, *26*, 1425−1435.
(8) Farkouh, A.; Riedl, T.; Gottardi, R.; Czejka, M.; Kautzky-Willer, A. Sex-Related Differences in Pharmacokinetics and Pharmacodynamics of Frequently Prescribed Drugs: A Review of the Literature. *Adv. Ther.* **2020**, *37*, 644−655.
(9) Smiderle, L.; Lima, L. O.; Hutz, M. H.; Van der Sand, C. R.; Van der Sand, L. C.; Ferreira, M. E. W.; Pires, R. C.; Almeida, S.; Fiegenbaum, M. Evaluation of sexual dimorphism in the efficacy and safety of simvastatin/atorvastatin therapy in a southern Brazilian cohort. *Arq. Bras. Cardiol.* **2014**, *103*, 33−40.
(10) Plakogiannis, R.; Arif, S. A. Women Versus Men: Is There Equal Benefit and Safety from Statins? *Curr. Atheroscler. Rep.* **2016**, *18*, 6.
(11) Raparelli, V.; Pannitteri, G.; Todisco, T.; Toriello, F.; Napoleone, L.; Manfredini, R.; Basili, S. Treatment and Response to Statins: Gender-related Differences. *Curr. Med. Chem.* **2017**, *24*, 2628−2638.
(12) Elsinga, P. H.; van Waarde, A.; Paans, A. M. J.; Dierckx, R. A. J. O. *Trends on the Role of PET in Drug Development*; World Scientific Publishing, 2012.
(13) Istvan, E. S.; Deisenhofer, J. Structural Mechanism for Statin Inhibition of HMG-CoA Reductase. *Science* **2001**, *292*, 1160−1164.
(14) Clemente, G. S.; Zarganes-Tzitzikas, T.; Dömling, A.; Elsinga, P. H. Late-Stage Copper-Catalyzed Radiofluorination of an Arylboronic Ester Derivative of Atorvastatin. *Molecules* **2019**, *24*, 4210.
(15) Clemente, G. S.; Rickmeier, J.; Antunes, I. F.; Zarganes-Tzitzikas, T.; Dömling, A.; Ritter, T.; Elsinga, P. H. [^{18}F]Atorvastatin: synthesis of a potential molecular imaging tool for the assessment of statin-related mechanisms of action. *EJNMMI Res.* **2020**, *10*, 34.
(16) Schachter, M. Chemical, pharmacokinetic and pharmacodynamic properties of statins: an update. *Fundam. Clin. Pharmacol.* **2005**, *19*, 117−125.
(17) Rees, S. Statins: All you need to know. *Nurse Prescribing* **2017**, *15*, 230−236.
(18) Kato, S.; Smalley, S.; Sadarangani, A.; Chen-Lin, K.; Oliva, B.; Brañes, J.; Carvajal, J.; Gejman, R.; Owen, G. I.; Cuello, M. Lipophilic but not hydrophilic statins selectively induce cell death in gynaecological cancers expressing high levels of HMGCoA reductase. *J. Cell Mol. Med.* **2010**, *14*, 1180−1193.
(19) Beckwitt, C. H.; Shiraha, K.; Wells, A. Lipophilic statins limit cancer cell growth and survival, via involvement of Akt signaling. *PLoS One* **2018**, *13*, No. e0197422.
(20) Melo, A. C.; Cattani-Cavalieri, I.; Barroso, M. V.; Quesnot, N.; Gitirana, L. B.; Lanzetti, M.; Valença, S. S. Atorvastatin dose-dependently promotes mouse lung repair after emphysema induced by elastase. *Biomed. Pharmacother.* **2018**, *102*, 160−168.
(21) Waxman, D. J.; Holloway, M. G. Sex Differences in the Expression of Hepatic Drug Metabolizing Enzymes. *Mol. Pharmacol.* **2009**, *76*, 215−228.
(22) van Bezooijen, C. F. Influence of age-related changes in rodent liver morphology and physiology on drug metabolism–a review. *Mech. Ageing Dev.* **1984**, *25*, 1−22.
(23) Lennernäs, H. Clinical Pharmacokinetics of Atorvastatin. *Clin. Pharmacokinet.* **2003**, *42*, 1141−1160.
(24) Thompson, G.; Morrell, J.; Wilson, P. W. F. *Dyslipidaemia in Clinical Practice*; Taylor & Francis, 2006.
(25) Human Protein Atlas, available from http://www.proteinatlas.org. Accessed march 2021.
(26) Mouse Genome Informatics, available from http://www.informatics.jax.org. Accessed march 2021.
(27) Expression Atlas, available from https://www.ebi.ac.uk/gxa/home. Accessed march 2021.
(28) Brotis, A. G.; Tsitsopoulos, P. P.; Paraskevi, T. M.; Tasiou, A.; Di Rocco, C.; Fountas, K. N. A hypothesis about the potential role of statin administration as adjuvant treatment in the management of Merlin-deficient tumors. *Interdiscip. Neurosurg.* **2014**, *1*, 11−15.
(29) El-Hajj, I. I.; Mourad, F. H.; Shabb, N. S.; Barada, K. A. Atorvastatin-induced severe gastric ulceration: a case report. *World J. Gastroenterol.* **2005**, *11*, 3159−3160.
(30) Shingaki, T.; Takashima, T.; Ijuin, R.; Zhang, X.; Onoue, T.; Katayama, Y.; Okauchi, T.; Hayashinaka, E.; Cui, Y.; Wada, Y.; Suzuki, M.; Maeda, K.; Kusuhara, H.; Sugiyama, Y.; Watanabe, Y. Evaluation of Oatp and Mrp2 Activities in Hepatobiliary Excretion Using Newly Developed Positron Emission Tomography Tracer [11C]Dehydropravastatin in Rats. *J. Pharmacol. Exp. Ther.* **2013**, *347*, 193−202.
(31) He, J.; Yu, Y.; Prasad, B.; Link, J.; Miyaoka, R. S.; Chen, X.; Unadkat, J. D. PET Imaging of Oatp-Mediated Hepatobiliary Transport of [11C] Rosuvastatin in the Rat. *Mol. Pharmaceutics* **2014**, *11*, 2745−2754.
(32) Yagi, Y.; Kimura, H.; Okuda, H.; Ono, M.; Nakamoto, Y.; Togashi, K.; Saji, H. Evaluation of [18F]pitavastatin as a positron emission tomography tracer for in vivo organic transporter polypeptide function. *Nucl. Med. Biol.* **2019**, *74*−*75*, 25−31.
(33) Lee, H. H.; Ho, R. H. Interindividual and interethnic variability in drug disposition: polymorphisms in organic anion transporting polypeptide 1B1 (OATP1B1;SLCO1B1). *Br. J. Clin. Pharmacol.* **2017**, *83*, 1176−1184.
(34) Ihedioha, J. I.; Noel-Uneke, O. A.; Ihedioha, T. E. Reference values for the serum lipid profile of albino rats (Rattus norvegicus) of varied ages and sexes. *Comp. Clin. Pathol.* **2013**, *22*, 93−99.
(35) Tomlinson, E. S.; Maggs, J. L.; Park, B. K.; Back, D. J. Dexamethasone Metabolism in Vitro: Species Differences. *J. Steroid Biochem. Mol. Biol.* **1997**, *62*, 345−352.

https://doi.org/10.1021/acs.molpharmaceut.1c00305
Mol. Pharmaceutics 2021, 18, 3378−3386